Image Modalities: Image registration

Daniel Barmaimon
Medical Image Analysis - Vibot Master
University of Girona

Abstract

The main purpose of this lab is to face the problems of registration. The choice of the geometrical model, the metric and the optimization method would be the main parameters to set. The understanding of the different options for each one of them, and the way to get the closer result it the target of this lab.

1. Introduction

Registration is the process of aligning a target image to a source image. More generally, determining the transform that maps points in the target to points in the source image. It will be an iterative process that has the

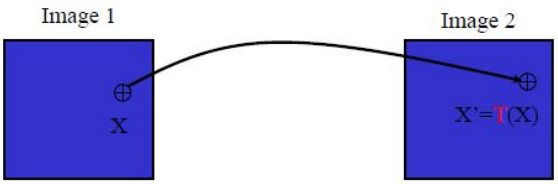

Figure 1: Registration process

schema shown in the following image. The are several

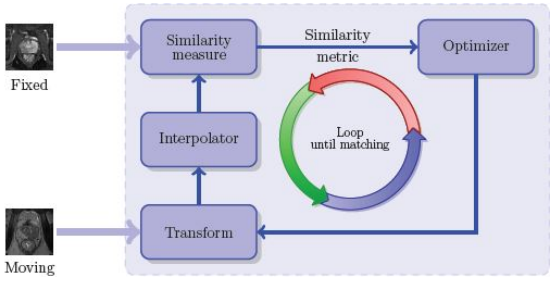

Figure 2: Registration schema

reasons to use registration in medical image analysis. The most important could be the following:

(a) Analysis of temporal evolution

(b) Fusion of multimodal images

(c) Inter-patients comparison

(d) Atlas superposition

(e) Reconstruction of a 3D volume

1.1. Analysis of temporal evolution

The ability to match images with different creation time allows the recognition of evolution of diseases and how treatment is working for each patient. With this information the doctor is able to diagnose better, change the treatment or estimate action times.

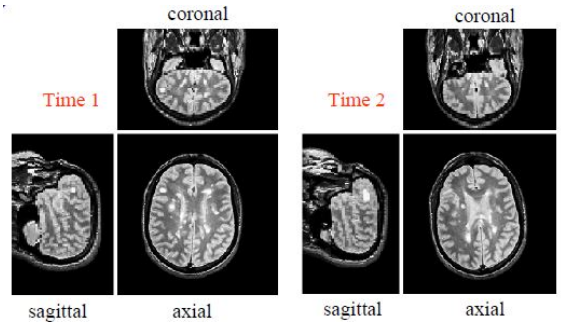

Figure 3: Registration process

1.2. Fusion of multimodal images

Most of the times there are details that could be better observed with not only one image acquisition method, but with several. Combination of MRI and PET is the most extended multimodal technique and allows doctor to see anything present in a specific tissue such as its size, location or metabolic activity.

1.3. Inter-patients comparison

Anomalies could be detected for patients who's images doesn't match with the average. For being able

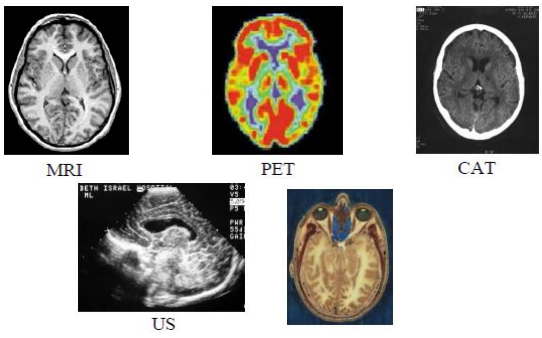

Figure 4: Multimodal image fusion and reconstruction of anatomical model

to do this kind of analysis is necessary to normalize the images, (avoiding differences in terms of sizes and distances). Computing statistics is possible to determine, for example, in the case of the brain variability, detection of diseases such as Alzheimer, AIDS/VIH, schizophrenia, drug abuse or evolution of a treatment.

1.4. Atlas superposition

Group of images that are acquired from different sites and/or at different times could be aligned simultaneously. The statistical information of this group of aligned images or the obtained from single images could be used to analyse anatomical shapes, create probabilistic segmentations, localize brain functional, etc.

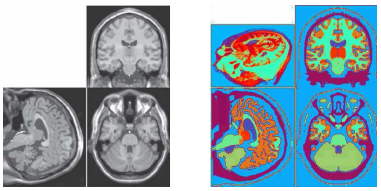

(a) MRI images (b) Labelled images

1.5. Reconstruction of a 3D model

A 3D model could be implemented by the reconstruction of several slices or projections if the registration between the images is well performed. Ultrasound, MRI or X-ray images allow this kind of reconstruction.

2. Kind of registration

There are two basic kind of registration depending on what it is wanted to be based. It could be based on

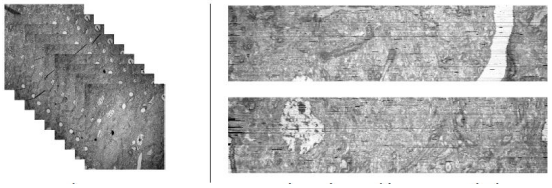

Figure 6: Series of successive 2D slices and orthoprojection of 3D reconstruction

features and is called *geometric registration*, or in intensity, *iconic registration* and *standard intensity registration*, or a combination of both of them.

2.1. Geometric feature based registration

GFB algorithms rely on a segmentation of part or all the images, done generally before the registration process itself. The segmented geometrical objects correspond generally to anatomical or mathematical invariants, like organ boundaries. Once extracted, these sets are registered by minimizing a set of correspondences C between points of the two sets. Then, a transformation T that interpolates or approximates these correspondences C is found using a geometrical distance between C and T as the distance function D to be minimized, and one model for the deformation. This model is needed because otherwise the motion of a point will be estimated independently of the motion of th neighbours).

2.2. Intensity based

2.2.1. Standard intensity based registration. The distance D between two images is one of the multiple similarity measures, such as squared difference, correlation coefficient, correlation ration, mutual information of the two images. The measure is compute between two points, one of each image, that are lying at the same position.

2.2.2. Iconic feature based registration. These algorithms pair points, lines or regions, according to their intensity, and fit geometrically a transformation to these pairings. This is a mix of the two previous methods.

3. Geometric transformation models

In this section it is going to be described the differences in the use of geometric models. The following images shown in Fig. 7 and Fig. 8 are the images that will be used to compute the registration.

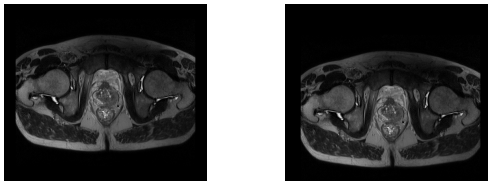

Figure 7: Original and translated images

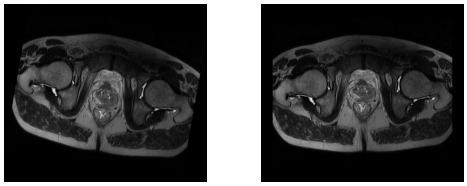

Figure 8: Rotated and distorted images

3.1. Translation model

In this iterative case the algorithm will measure the differences between the two images assuming that all the pixels have the same displacement. The optimizer will be tuned up with a minimum and a maximum step distances, a stop condition that could be a maximum number of iterations or a threshold for the distance between the images and the initial offset for X and Y coordinates. In the case of choosing the total number of iterations as condition for stopping, the algorithm will store the best result during the process, returning it at the end after all the iterations without taking care if the best value was acquired at a very early iteration. On the other hand, taking the threshold as the stopping condition could lead into an infinite loop if the threshold is too low, or if the image is not only translated but also deformed in some other way (rotated, scaled, etc.) because the distances between the images in each iterator is never lower than this threshold.

3.1.1. Translation. The results obtained for the difference between the two original images, before starting, and after the process are shown below. The

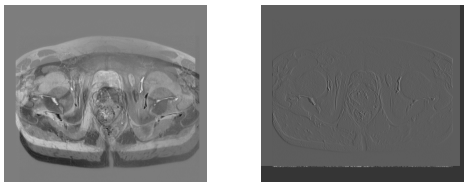

Figure 9: original-translated, original-output

only appreciable difference between the output and the original image is in the border of the image because of the shift. A little bit of the contour could be also seen but this is negligible comparing with these border. For avoiding to take into consideration these borders in the computation of the distances is better to select a *ROI*, region of interest at the beginning.

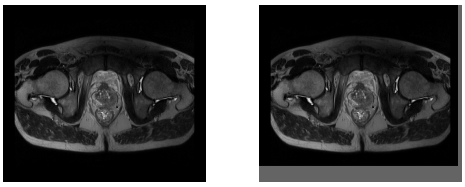

Figure 10: Original and output for translated images

3.1.2. Rotation. If the differences obtained with this model for a rotated image are analyzed, the results are not so good. In this occasion the point where the rotation axis is located will be the only one that is well located.

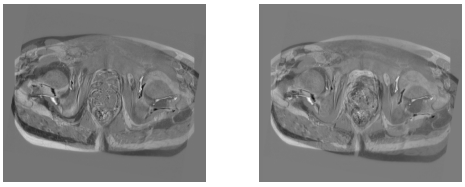

Figure 11: rotated-translated, rotated-output

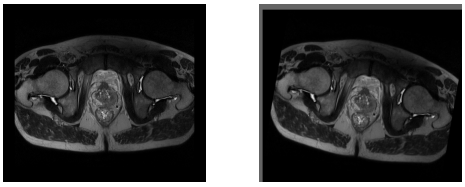

Figure 12: Original and output for rotated images

3.1.3. Distortion. Distorted part it's seen with blur or overlapped. The model appears to work fine for non-distorted part, but that means nothing because that part will remain as the original one.

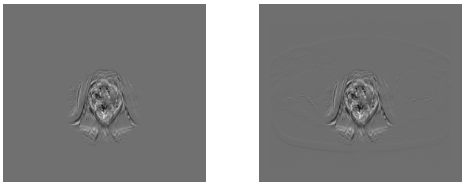

Figure 13: distorted-translated, distorted-output

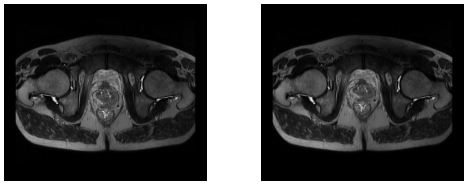

Figure 14: Original and output for distorted images

With this model no transformation will be implemented over the distorted image, independently of the tune up of the parameters of the optimizer.

3.2. Affine model

The model purpose an affine transformation for each pixel. Assuming $\varphi$is linear and applicable for each point $x \in \mathbb{R}^2$:

$$\varphi(x) = \begin{bmatrix} a_{11} & a_{12} \\ a_{21} & a_{22} \end{bmatrix} \begin{bmatrix} x_1 \\ x_2 \end{bmatrix} + \begin{bmatrix} t_1 \\ t_2 \end{bmatrix} = Ax + b \quad (1)$$

The matrix A of this linear transformation could be expressed as follows.

$$A = \begin{bmatrix} cos\theta & -sin\theta \\ sin\theta & cos\theta \end{bmatrix} \begin{bmatrix} s_{x1} & 0 \\ 0 & s_{x2} \end{bmatrix} \begin{bmatrix} 1 & S_{x1} \\ 0 & 1 \end{bmatrix} \quad (2)$$

where is each matrix corresponds to a rotation, a scale and a shear receptively. This with the complement of the translation given by the vector b makes this model one of the most used for registration in medical image.

3.2.1. Translation. The results for the translation in the affine model are shown in Fig. 15 and Fig. 16.

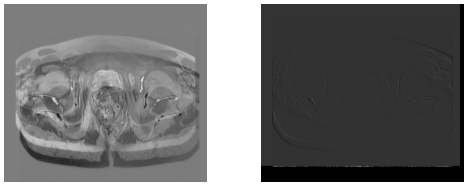

Figure 15: affine-translated, affine-output

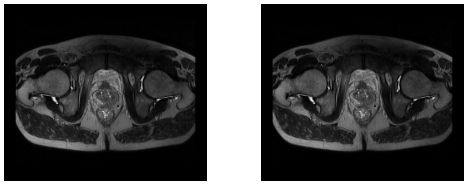

Figure 16: Original and output for translated images

3.2.2. Rotation. The results for the rotation in the affine model are shown in Fig. 17 and Fig. 18.

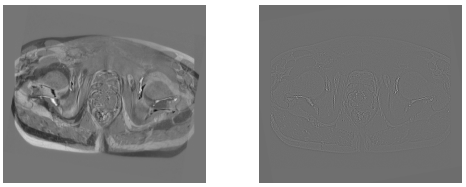

Figure 17: affine-rotated, affine-output

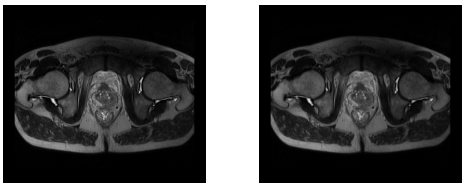

Figure 18: Original and output for rotated images

3.2.3. Distortion. The results for the rotation in the affine model are shown in Fig. 19 and Fig. 20.

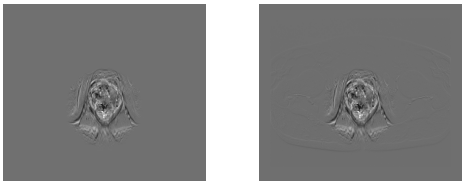

Figure 19: affine-distorted, affine-output

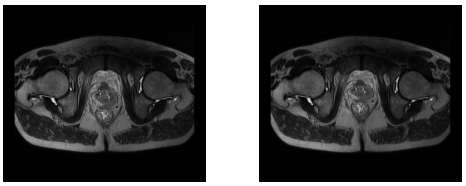

Figure 20: Original and output for distorted images

After checking all the results for the images the conclusion is that this transformation is much better that the obtained for the translation model. It is much better for the rotational model but still not responds well for distorted images.

3.3. B-spline model

In this case the model will be defined by basis splines. To understand the concept it is necessary to describe a function as a combination of basis functions.

$$v(x) = p_i \beta_i(x) \quad (3)$$

where β_i is a piecewise cubic polynomial and p_i is a scaling factor for each spline. Due to their many desirable properties such as local control, smoothness, and computational efficiency, cubic B-spline surfaces are widely used in surface modeling. In free form deformation, they (or, rather, their volumetric generalizations to volumes) may be used by embedding an object into a B-spline volume and then changing the shape of the object by moving the B-spline control points as is shown in Fig. 21 The process will measure the displacement

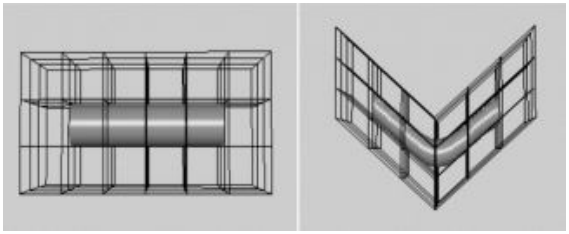

Figure 21: Free form deformation

between pixels of the two images with similar intensity values. This process will be iterative until achieve the best possible result. Over the fixed image the process will map the vectors, that corresponds with the displacement of each pixel, as it is illustrated in th Fig. 22

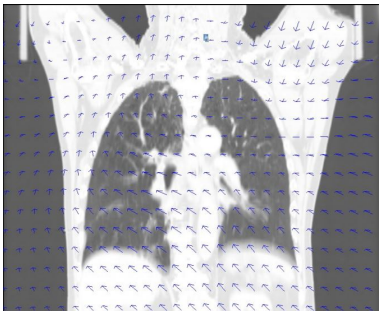

Figure 22: Vector field over original image

Usually the higher the degree of the b-spline the higher the smooth of the image and the higher the computational time. That's why is quite popular the use of cubic splines.

The images that are going to be used for this section are represented in Fig. 23 and Fig. 24 .

3.3.1. Translation. The results for the translation in the affine model are shown in Fig. 25 and Fig. 26.

3.3.2. Rotation. The results for the rotation for this model are shown in Fig. 27 and Fig. 28.

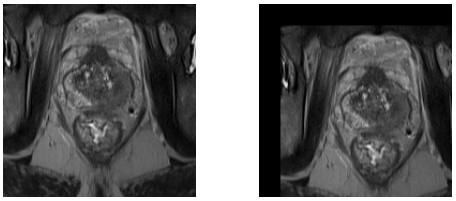

Figure 23: Original and translated images

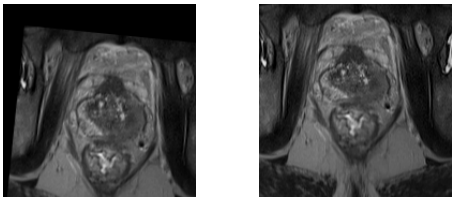

Figure 24: Rotated and distorted images

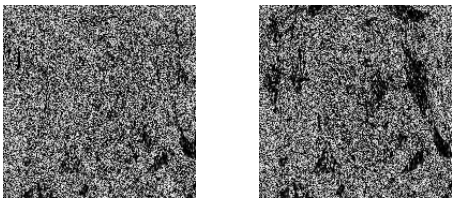

Figure 25: bsplines-translated, bsplines-output

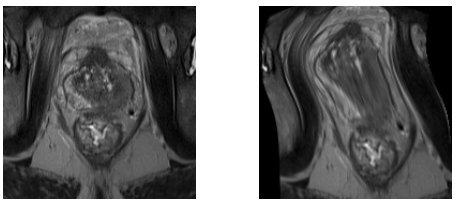

Figure 26: Original and output for translated images

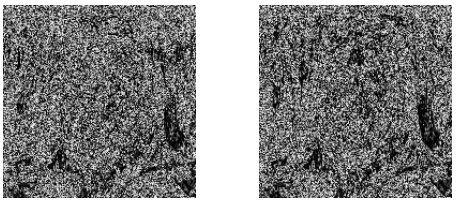

Figure 27: affine-rotated, affine-output

3.3.3. Distortion. The results for the rotation in the affine model are shown in Fig. 29 and Fig. 30. The results weren't good for the translated and rotated images, but it was for the case of the distorted image. This was expected because non-rigid transformation method work better with deformed images.

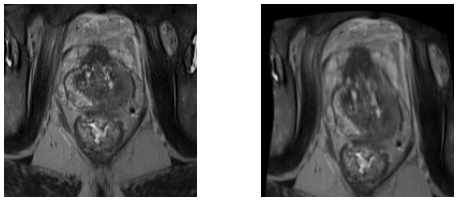

Figure 28: Original and output for rotated images

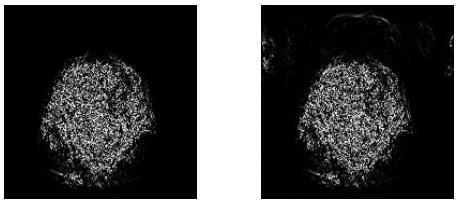

Figure 29: splines-distorted, splines-output

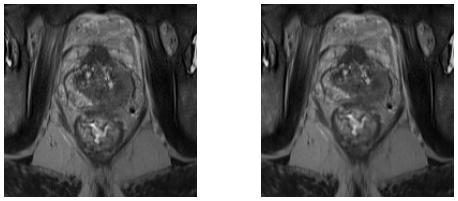

Figure 30: Original and output for distorted images

4. Similarity metrics

This section will collect the results of using different metrics and the comparison between them. The metrics that will be analyzed are *mean squared difference* and *mutual information-based*.
There will be two experiments to be represented for each metric, and the images and the original images for are shown below in Fig. 31.

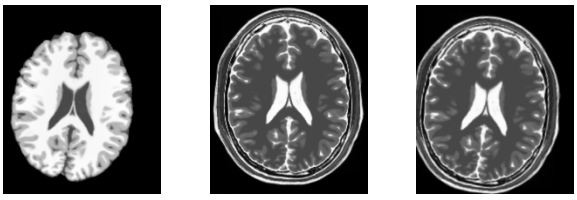

Figure 31: Image1, Image2 and Image2 moved

4.1. Mean squared difference metric

The metric will compare the intensity of two pixels. A normalization factor should be use to compare level of similarities of two different pair of images.

$$RMS(A,B) = \frac{1}{N}\sqrt{\sum_{x=0}^{X}\sum_{y=0}^{Y}(A(x,y)-B(x,y))^2} \quad (4)$$

For this case only level of gray between the pixels is measured and this will be reflected in the results. The

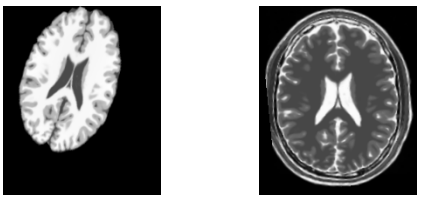

Figure 32: Registered images 1 and 2

first registered image isn't aligned at all, and that is reflected on the metric gotten, 11967. The second one is well aligned and only is lost the part that is missing in the moved image. The metric in this case is 92. As conclusion it is possible to say that this metric is not a good choice for multi-parameter images.

4.2. Mutual information-based metric

Mutual information is an information theory measure of the statistical dependence between two random variables or the amount of information that one variable contains about the other. It can be qualitatively considered as a measure of how well one image explains the other. It assumes a statistical relationship that can be captured by analyzing the images' joint entropy. For understanding how is possible to measure the similarity with entropy data is necessary to introduce the concept of joint entropy *H(A,B)*.

$$H(A,B) = -\sum_{a,b} p_{AB}(a,b) log_{p_{AB}}(a,b) \quad (5)$$

This joint entropy will be minimized when there is a one to one mapping between the pixels in A and their counterparts in B. It will rise up when the relationship between A and B starts to be weaker. Mutual information considers both the joint entropy *H(A,B)* and the individual entropies *H(A)* and *H(B)*, as is shown in the formula below.

$$H(X) = -\sum_{x} p_X(x) log_{p_X}(x) \quad (6)$$

Finally is possible to define mutual information as follows.

$$MI = H(A) + H(B) - H(A,B) \quad (7)$$

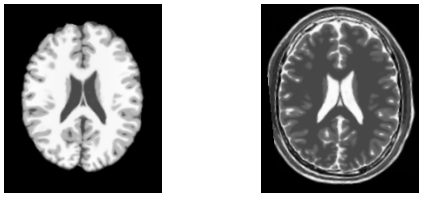

Figure 33: Registered images 1 and 2

The results for the two images are shown in Fig. 33 In this case the registration worked fine both for multi-parameter and for mono-modality images. In this case the values for the metrics were 0.81 and -1.43, respectively.
The times between for the registration of second image with different metrics is almost the same. For the first image MSD reach the maximum number of iterations without a good result so it has no sense to compare the times. The two metrics studied could not be compared quantitatively but it has been demonstrated that they work equally good for mono-modality images. Only MI based metric works properly for multi-parameters images.

5. Method for interpolation

The registration process matches two images with similar characteristics that are set in different positions. Normally these distances between pixels are not integer numbers, so is needed to use methods to interpolated the values of the gray levels according to different criteria. The methods that are going to be introduced in this report are *nearest neighbours* and *B-spline* interpolations. The images that are going to be used to analyzed the methods are shown in the Fig. 34

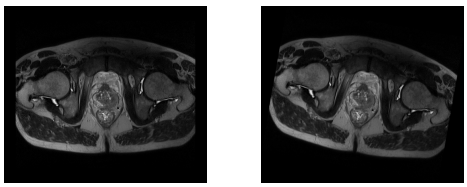

Figure 34: Original and rotated images

5.1. Nearest neighbours interpolation

The method consist in approximate of the value of the gray level of the pixel to the one that corresponds to the nearest neighbour. In the Fig. 35, the nearest neighbour for the position *E* would be *G*. The result obtained in this case for the final image is shown in the Fig.. 36

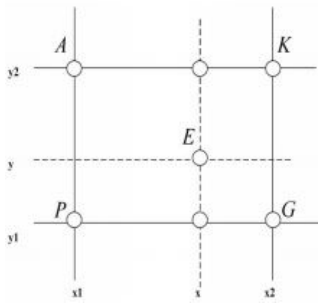

Figure 35: Four neighbours around an empty position

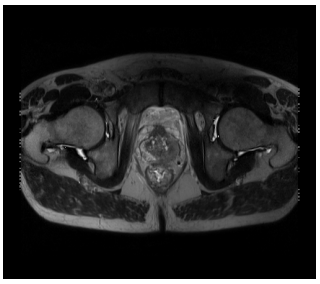

Figure 36: Resulting image for NN interpolation

5.2. B-spline interpolation

This method uses the B-splines to interpolate. This kind of functions have been explained in section 3.3. The result obtained for this method is shown in Fig. 37 To appreciate in a qualitative way the interpolation effect is need to zoom a little to check the difference between the two methods. As it could be seen in the Fig. 38 the interpolation that better fits is B-splines. A quantitative analysis is shown in the following table.

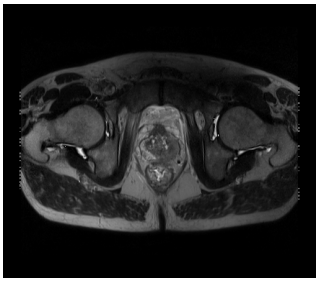

Figure 37: Resulting image for B-spline interpolation

Method	Time	Iter.	Metric	SSE	C. C.
NN	13.071	90	-1.0475	185015	0.9981
B-spline	2.19	69	-1.128	124848	0.9987

The computation time for B-splines is much greater than in the case of nearest neighbours, but the number

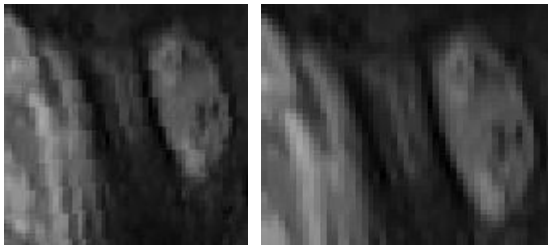

Figure 38: NN and B-splines interpolation details

of iterations is lower; so it means, that B-splines takes much more time for each iteration than NN. The metrics are quite similar and not far from zero, what means that the similarity achieve is acceptable in both method. A qualitative way to analyze the registered images could be to compare the sum of squares error. As a conclu-

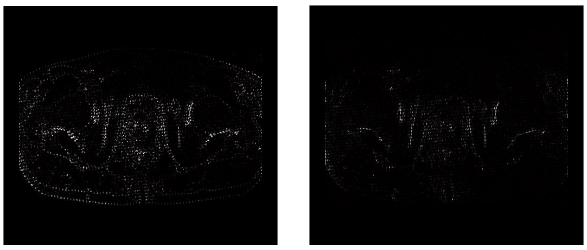

Figure 39: NN and B-spline sum square error images

sion it is clear that the error for b-spline interpolation is much more smoothed and the definition of the edges looks more defined.

6. Optimizer

The differences in the tuning of the optimizer could lay to different results, iterations and computational time. Several experiments were performed to understand the behaviour of the algorithm with some changes in the optimizer parameters. For each experiment collected in the table a curve on the graphic could be found. This curves represent the error for each iteration once the parameter were set. The are collected in the following table.

Exp.	Max n iter	Max step	Min step
1	300	0.1	0.0001
2	300	0.5	0.0001
3	300	0.1	0.0000001
4	500	0.1	0.0001
5	50	0.1	0.0001
6	50	1	0.0001

The representation of the error after each iteration for each experiment is shown in Fig. 40

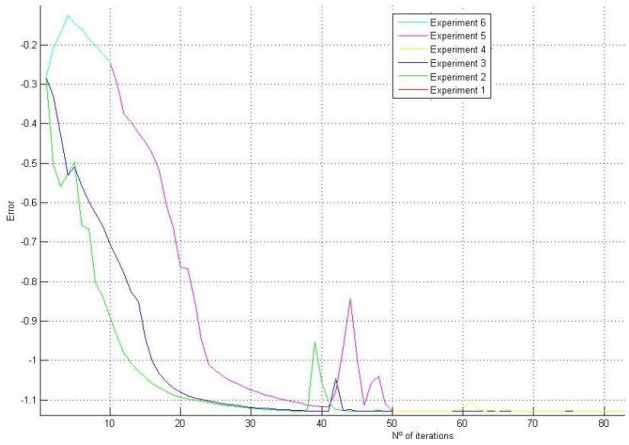

Figure 40: Evolution of error versus iteration number

In this case a smaller step get a quicker response as is could be seen in experiment 3 (minimum step 0.0000001). A greater maximum step give a quick response too and stabilize even with short number of iterations, like in experiment 6.

This analysis should be done for each particular case, obtaining an customized set up for each of them.

7. Full registration

This last part of the report will contain the result of the evaluation method for four different patients using the same parameters in the registration process. First thing that could be done is to check the result of DICE coefficient and the overlapping of the images (original and registered) after the process.

Experiment	DICE	TRE (mm)
1	0.66122	9.43
2	0.87378	2.4295
3	0.94221	0.51536
4	0.62372	11.0059

The parameters used in this case were an affine model, with mattes mutual information metric and B-splines interpolator. It is seen graphically in the Fig. 41 that the registration is better for the third patient images and same could be done numerically because is the one with the greater DICE coefficient and the lower TRE distance. For the rest of the images the recommendation will be to modify the parameters used in order to achieve better results.

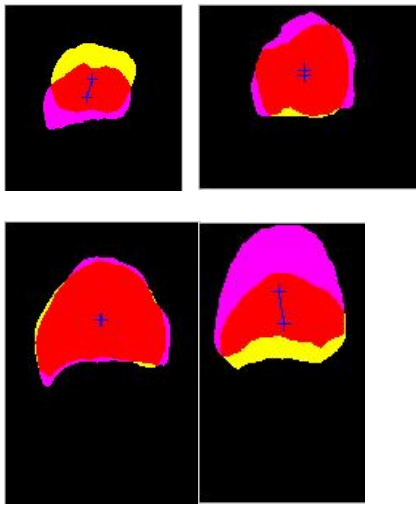

Figure 41: Result images with TRE of different patients and same parameters

References

[1] ”Automatic Detection and Segmentation of Evolving Processes in 3D Medical Images: Application to Multiple Sclerosis. Medical Image Analysis, 6(2):163-179”, David Rey, Grard Subsol, Herv Delingette and Nicholas Ayache. June 2002

[2] ”Fundamentals of Medical Imaging Registration I-II”, Oliver Clatz Ph.D., Harvard University

[3] ”Medical Imaging: Technology and Applications”, Lisa Tang and Ghassan Hamarneh , 2013

[4] ”A robust affine image registration method”, Noppadol Chumchob, Ke Chen, International journal of numerical analysis and modeling, 2009

[5] ”Handbook of Medical Imaging: Medical image processing and analysis”, J. Michael Fitzpatrick, Derek L. G. Hill, Calvin R. Maurer, Jr.

[6] ”Computer Vision - ECCV 2004”, Daniel Russakoff, Carlo Tomasi, Trsten Rohlfing, Calvin R. Maurer, Jr., Department of Computer Science, Standford University, 2004

[7] ”Image Registration Using Hierarchical B-Splines”, Zhiyong Xie, Gerald E. Farin, IEEE Transctions on visualization and computer graphics, vol 10, n1, january/february, 2004

[8] ”Lecture notes - Medical Image Analysis”, G. Lematre, R. Mart and J. Mart, Universitat de Girona, 2014